Consolidation of
Nanoscale Iron Powders

Z. Livne and A. Munitz
Nuclear Research Center Negev
Beer-Sheva, Israel

J. C. Rawers
U.S. Dept. of Energy
Albany, OR 97321

R. J. Fields
Metallurgy Division
NIST
Gaithersburg, MD 20899

NIST

Consolidation of Nanoscale Iron Powders

Z. Livne and A. Munitz
Nuclear Research Center Negev
Beer-Sheva, Israel

J. C. Rawers
U.S. Dept. of Energy
Albany, OR 97321

R. J. Fields
Metallurgy Division
NIST
Gaithersburg, MD 20899

March 27, 1997

Consolidation of Nanoscale Iron Powders

Z. Livne[1], A. Munitz[1], J. C. Rawers[2], and R. J. Fields
Metallurgy Division, NIST

Abstract

The consolidation behavior of two types of nanoscale iron powders, vacuum condensed (nanograins in nanoparticles) and ball-milled (nanograins in microparticles) was studied. For comparison, the consolidation of two microscale powders, atomized and ground, was also characterized. Consolidation techniques investigated were cold closed die compaction, cold isostatic pressing (CIPing), and, after CIPing, sintering or hot isostatic pressing (HIPing). The mechanical properties, density, and microstructure of the resulting compacts were found to depend on the type of powder, and its consolidation history. Significant differences in behavior were found between the microscale and nanoscale powders. An additional reason, besides the dissimilarity in grain size, for these differences was the fact that the two nanograin powders contained significant amounts of oxygen which ultimately resulted in a distinctly two phase bulk microstructure. The vacuum condensed powder achieved satisfactory green strength on CIPing and high hardness (440 H_V - Vickers hardness) on low temperature sintering. While not necessary for complete consolidation, HIPing at 500 °C was found to be beneficial and compacts of this powder were found to have a hardness 0f 680 H_V and a high compressive yield strength (1800 MPa). For ball-milled powders HIPing was found to be essential for effective consolidation. For example, the ball-milled material, which remained friable after CIPing and sintering at 580 °C, achieved extremely high hardness (820 H_V) when HIPed at 580 °C and a pressure of 175 MPa. Its ductility was greatly improved when HIPed at temperatures between 700 °C and 850 °C, while preserving its relatively high strength. The behavior of these nanoscale powders can be understood by considering the three most important processes taking place during the consolidation of any powder: densification, particle bonding, and grain growth. Optimization of these processes may result in unique mechanical properties of the ball milled powders. It was found that these three processes are strongly influenced by the grain size and particle size of the powders investigated, and oxidation level.

---

[1]Visiting Scientists at NIST on leave from the Nuclear Research Center, Negev, Israel.
[2] Dept. of Energy (formerly Bureau of Mines), Albany OR.

1) Introduction

Interest in nanoscale materials has increased in recent years with the realization that unique properties may be obtained from otherwise ordinary materials[1-3]. This idea arose from an extrapolation of known grain size effects to nano-grain sizes where such effects are not known to be valid[4,5]. The availability of nanoscale materials in reasonable quantities to manufacture bulky bodies would make the experimental evaluation of such predictions possible.

Another reason for interest in nanoscale powders often stated in the literature on these materials[4] is that they may consolidate more readily or more completely than conventional powders. The high specific surface area provides a significant driving force for densification. The extremely fine grain size provides an additional mechanistic route (diffusive flow by Nabarro-Herring or Coble creep) for densification that is available to coarser powders only at extremely high temperatures. Under such conditions, coarsening and pore trapping become severe problems. Coarsening is still an issue even at the more moderate temperatures required to densify nanoscale materials. If the object is to produce dense, nanocrystalline materials, sintering or HIPing temperatures and times must be chosen so as to maximize density and interparticle bonding, and minimize coarsening.

The present research was undertaken to optimize the sintering and HIPing of nanoscale powders to obtain bulk nanocrystalline materials for mechanical properties evaluation, and to find out the impact of particle and grain size effects on the mechanical properties.

2) Experimental Procedures

The consolidation behavior of two types of nanoscale iron powders was studied. One powder consisted of nanoscale grains in nanoscale particles produced by vapor condensation (NN, for nano-nano). The other powder consisted of nanoscale grains in micrometer scale particles produced by ball milling (NM, for nano-micro). For comparison the consolidation of two microscale grain/microscale particles (MM, for micro-micro) produced by atomization (MMa) and grinding (MMb) was also characterized. Consolidation was accomplished by a combination of standard techniques including cold closed die pressing, cold isostatic pressing (CIPing), and, after CIPing, sintering or hot isostatic pressing (HIPing). First, the powder was insert in a cylindrical rubber CIPing bags than CIPed to 350 MPa. The entire cycle took about 5 minutes with about 15-30

seconds at maximum pressure. Usually, the powder was initially loose in the bag, but, in the case of the NN powder, tamping by hand to about 20% relative density was necessary to achieve a reasonably sized final compact.

Cold closed die pressing was carried out in a special apparatus developed at NIST[6] . In essence, it consisted of a carbide cylinder in a steel cylindrical sleeve and two carbide push rods. The compressive force was applied to the push rods by a standard, screw-driven, mechanical testing machine. The actual force applied to the powder was determined using a double load cell system that measured and subtracted any load shedding to the cylinder. In each case a known amount of loose powder was introduced into the cylinder with the lower rod in place. The upper rod was inserted and the pressure applied.   The change in the volume of powder was determined from the measured displacement of the push rod.

Sintering of previously CIPed samples was carried out in a vacuum furnace. The vacuum ranged between 0.5 Pa and 1.0 Pa. Heating to the desired sintering temperature usually took about half hour and control was ±5 °C. In some cases, heating in flowing hydrogen was used to reduce the oxide layer on the iron particles of previously CIPed samples. The procedure employed for deoxidization consisted of first evacuating the chamber to a pressure of 0.5 Pa to 1.0 Pa range at room temperature for 20 hours. The chamber was then back filled with a flowing argon/5% hydrogen mixture at a pressure of one atmosphere. The temperature would then be raised to 375°C for 24 hours.

Hot isostatic pressing (HIPing) of the CIPed compacts was performed in a commercial HIP unit. The compacts were first canned in copper tubes which were then evacuated to 10 Pa and sealed by electron beam welding. They were then placed in the HIP unit and heated to the desired temperature for three hours in pressurized argon gas. The pressure used for HIPing was in every case 175 MPa. After HIPing, the copper cans were removed by machining.

After consolidation, the compacts were characterized by optical and scanning electron microscopy, and density measurements.

The apparent tap density measurements were obtained by weighing known volumes of tapped powder. The densities of porous compacts were determined by weighing machined cylinders of known volume. In cases where the bodies were no longer porous to water, the volume was determined by measuring the volume of water displaced by the body.

Mechanical properties characterization involved hardness measurements and compression tests. Vickers hardness tests were done on polished

metallographic samples using a load of 300 grams for about 12 s. The compression tests were run on a screw-driven mechanical test machine at a cross head speed of 0.02 mm/s. For these tests, cylindrical samples, 5 mm in diameter and 9 mm long, were compressed between carbide platens. Load and displacement data, collected during the test, were later converted to stress and strain.

3) Results
3.1) Powder Characterization:
The starting powders were nominally pure iron which contained varying amounts of oxygen. While oxygen may be thought of as an impurity, it is often intentionally added to deactivate the surface and reduce flammability or explosion hazards associated with fine powders. The oxygen contents of the NN, NM and MM powders are listed in Table 1. Both MM powders contained negligible amounts of oxygen. The morphology of the as-processed powders are presented in Figures 1a to 1d. As seen in the figures, the powder particles and grain size ranged from nanoscale grains in nanoscale particles (NN powder) to tens of micrometers grains in tens of micrometers particles (MM powder). The actual sizes are also listed in Table 1, together with their designation. The different powders could readily be distinguished by their apparent relative density which ranged from less than 10% (similar to snow) for the NN powder to 43% for the MM powders(Table 1). The finer the particles size of the powder, the lower its apparent density.

3.2) Consolidation Behavior:
All powders were cold isostatically pressed (CIPed) to 350 MPa in rubber bags. The resulting densities of consolidated bodies of the different powders are shown in Figures 2a, to 2c, respectively. After cold consolidation, the NN, MM(a), and MM(b) compacts were found to hold together fairly well. The NM powder did not CIP well: compacts were friable and returned to powder by rubbing between the fingers. To ascertain whether higher pressures were needed to raise the green strength of NM consolidated bodies, it was cold pressed in a closed die [6] to 2.5 GPa. For comparison, MM(a) was also pressed in the same system. The density versus pressure curves are shown in Figure 3. The density of the MM(a) powder increase with increasing pressure Increasing pressure up to 1.5 GPa, where it level of at a value of 95% the theoretical density. Further pressure

increasing to 2.5 GPa bring the density to almost the theoretical density while obtained nice solid body. In contrast, the curve for the NM powder did not level off even at the maximum pressure used of 2.5 GPa and the density reached only around 75% of the theoretical density value. Even after application of this high pressure, the resulting pellet was still friable and could be returned to a powder by rubbing.

The densification due to CIP followed by sintering is compared to HIPing in Figure 2. Sintering for three hours at different temperatures resulted in some density increases. The nanoscale powders' densities depend strongly on sintering temperature until the highest density is reached. For example, NN reached its highest density after sintering at 850 °C for three hours. As expected, HIPing results in higher densities at lower temperatures than sintering. For example, HIPing NM powders at 580 °C and 175 MPa for 3 hours reached its highest density whereas, by sintering for 3 hours, it had not reached the same density even at a temperature of 965 °C. The resulting density from some of the treatments is summarizes in Table 2a to 2d.

3.3) Microstructure:

The microstructures of consolidated NN powder (CIPed and sintered to different temperatures) are shown in Figures 4a through 4d. Microhardness indentations are also seen in these photomicrographs. Sintering above 500 °C caused oxide particles precipitation. The amount and size of the precipitates increased with increasing sintering temperature. AT 965 °C, an interconnected dual microstructure of iron (light phase) and oxide (dark phase) was observed. As we shall see later, oxide precipitation was observed also in NM powders after sintering at temperatures above 700 °C but in lower densities levels than the NN powder.

3.4) Mechanical Properties:

The hardnesses of NN, NM, and MM(a) consolidated by HIPing or CIPing and then sintering to different temperatures are given in figures 5a, 5b, and 5c, respectively. Clearly, the hardness of NN increased dramatically on low sintering temperature (500 °C). In contrast, the NM powder was so weak that reliable hardness data could only be obtained on material sintered at or above 700 °C. Under these sintering conditions, NM was only slightly harder than the as-CIPed powder. HIPing, however, greatly improved NM's hardness, making it much harder than NN.

The compression stress-strain curves for NN, NM, and MM(a) as a function of the process variables are presented in figures 6a, b, and c, respectively. MM powder compacts shows extensive ductility for all the sintering temperatures. In contrast, at low sintering temperatures (580 °C), the hydrogen reduced NN bodies had high strength (1125 MPa), but low ductility. As the sintering temperature increases to 850 °C, the ductility of NN improved to 17 % with a loss in strength to 840 MPa. Oxide reduction treatments carried out on NN effected a decrease in the yield strength, the ultimate compressive strength, and increase the amount of plastic deformation before compressive failure at any given processing temperature. The general mechanical properties behavior with processing temperature was similar to untreated NN except that the peaks in the mechanical properties occurred at lower temperatures.

The sintered NM bodies were, for most sintering conditions, weaker than conventional powder compacts with no ductility at all. At fairly high sintering temperatures (>900 °C) it behaves was similarly to conventional powder compacts. In contrast, HIPing of NM compacts improved the mechanical properties as illustrated in Figure 7 and in Table 2b.

Examples of ductile, partially brittle, and completely brittle fracture of the cylindrical compression test samples are given in Figure 8. Brittle bodies brake into many pieces (Figure 8c), while partially brittle fracture brake into two pieces. In contrast, ductile bodies did not brake. The diameter of the ductile sample increased while the length decrease. Fractography of the test samples supported the above observations.

In Figure 9, the fracture surface for NM sintered at 700 °C may be compared with those HIPed at 580 °C, 700 °C, and 850 °C. The original particles are still visible in the sintered body and little evidence of bonding can be seen. The HIPed samples show evidence of complete bonding and the fracture surface consisted of transgranular shear rupture (dimples) fracture at HIPing temperatures of 700°C and above. There are particles inside the dimples which were identified by microprobe analysis as oxygen rich particles. Therefore, they may be oxides. The oxides size increased in with increasing consolidation temperature, which in turn caused an increase in the dimples size with increasing temperature.

In figure 10, fractographs of NN sintered to different temperatures (a, b, and c) and HIPed at 500 °C (d) are presented. As can be seen from the figures, the fracture surfaces of the sintered NN bodies at 700 °C and the HIPed NM

materials at 700 °C have similar morphologies, i.e. dimples structure. This fact suggests that sintering NN powders is sufficient to promote bonding.

The fracture morphology of sintered MM(a) is presented in figure 11. The original powder particles could be seen on fracture surfaces of material sintered at 580 °C. No original powder particles could be observed when sintered at 700 °C. This suggest that densification and bonding of the MM powders occur at sintering temperatures below 700 °C .

4) Discussion
4.1) General
The present research evaluates the ability of different consolidation routes to produce fully dense and well bonded nanoscale iron bodies from two types of nanoscale powder (nano-grains in nano-particles-NN, and nano-grains in micro-particles-NM). While densification mechanisms relying on diffusion may be greatly accelerated at relatively low temperatures by small particles and fine grain size, it is necessary to achieve some initial compaction with finely dispersed porosity and an intimate contact between most of the powder particles before these mechanisms become effective. This is usually accomplished by pressing the fine powder to cause particle rearrangement and plastic compaction. It is at this stage that ball milled powders (NM powder) present consolidation difficulties. The NM particles are approximately the same size as the MM(a) powder, but with nanograins the particles are extremely hard, presenting much greater resistance to plastic deformation. Only HIPing allows densification of NM powder to proceed because the material becomes much softer with increasing temperature and grain growth. In contrast, for nano-grains in nano-particles (NN powder) the grain size is larger than the NM grain size (see table 1) and is thus softer than the NM powder. The finer particle size also reduces the pore size. As a consequence, particle rearrangement caused by CIPing is sufficient to make densification by curvature-driven bulk diffusion effective for eliminating the resulting fine porosity during sintering. If heat and pressure are applied (i.e., HIP), a further modest densification occurs compared to CIPing and sintering. In addition, CIPing followed by sintering of NN powders at 500 °C for 3 hr caused an increase of the hardness from 135 H_V of the as CIPed to 439 H_V, while HIPing for the same time and temperature raised the hardness to 515 H_V. In contrast CIPing followed by sintering of NM powders at 580 °C for 3 hr did not change the hardness of the CIPed body (around 110 H_V) while HIPing increased the hardness to 820 H_V.

It is possible to achieve densification without good bonding between particles especially at low temperatures. While cold welding has been demonstrated in some systems[7], good bonding between particles of most materials occurs at elevated temperatures where diffusion is significant. However, the rate of grain growth also depends on diffusion and hence, on temperature. Therefore, the achievement of a fully dense material with nanoscale grain size and associated properties requires careful consideration of how densification, bonding, and coarsening respond to the consolidation conditions in each particular powder.

4.2) The relationship between density, hardness, strength, and ductility

The main tests used here to study the combined effects of densification, bonding, and coarsening are hardness and uniaxial compression. The hardness of the consolidated body takes into consideration not only the hardness of the material but also the porosity level of the materials [5,8,9,10]. Therefore, for example, inspite of the fact that the hardness of the individual particles in the ball-milled powder (NM) exceeds 1000 H_v[8,11] the hardness of the CIPed powders that are sintered below 850 °C is very low (around 110 H_v) due to the porosity content and lack of bonding. In contrast, HIPing at temperatures above 500 °C increases markedly the hardness as well as the density. For example, the hardness of a body HIPed at 370 °C is 240 H_v while the hardness increased to 840 H_v when HIPed at 500 °C. At the same time the density increased from 5.9 g/ml to 7.1 g/ml, compared to the theoretical density (including the oxides) of 7.6 g/ml. This indicate that a major portion of the pores has been eliminated. In the case of Cold Dynamic Compaction (CDC) the densities of those powders[11] reached about 7.3 to 7.4 g/ml, while retaining the grain size similar to the as processed powder and keeping the work hardening of the ball milled powder. This, in turn caused the hardness to increase 1300 H_v.

High density and hardness does not imply necessarily the existing of bonding between the particles. For instance, the compression test of a specimen HIPed at 500 °C resulted in a fracture without any plastic strain at all. This means that due to the consolidation techniques (HIP at low temperatures) the hard particles came into intimate contact (high density) but only with partial bonding. Essentially, the hardness test gives some measure of the plastic flow properties, but it correlates with the density more than with the

degree of bonding. The uniaxial compression test measures the compressive strength in the case of a brittle material. For more ductile materials, it measures the plastic yield strength and work-hardening behavior, and gives some indication about the ductility. This ductility level provides insight into how well the particles have bonded together.

4.3) The role of oxygen in powder consolidation.

It is important to remember that the nanograin materials studied here always contain a significant amount of oxygen present as iron oxide. Full density for the nanoscale materials is therefore somewhat less than that for pure iron (7.6 gm/ml) because iron oxide is less dense than iron. This hard, oxide phase strengthens the resulting composite considerably, affects the consolidation behavior, and complicates comparisons between the nanograin material and more conventional iron compacts. It is possible to make nanograin iron powder without oxygen and some researchers[8] are doing it. However, the handling problems associated with oxygen-free iron are considerable and it is likely that the passivated material studied here is of greater commercial interest. The densification of hydrogen reduced nanoscale materials are shown on figure 2. Although reduced NN compacts are denser than the unreduced ones, metallography reveals some small amount of oxide remaining in the hydrogen reduced materials. The increase in density was accompanied with hardness decrease associated with the reduction in oxide content..

The amount of oxygen in the different powders might influence the consolidation behavior in three ways: (i) very fine precipitates of oxide might have a greatly increase the particles' strength; (ii) bonding might be hindered by the presence of oxides on the particle surfaces; and (iii) oxide might limit or reduce grain growth. The effect of oxygen on grain growth and strengthening is now under investigation.

4.4) Hall-Petch relationship

The fully dense samples produced in this study have grain sizes of 100 nanometers and up. It is appropriate to use these as a test of whether the Hall-Petch relation can be extrapolated to such fine grain sizes[12, 13]. Figure 12 shows the dependence of hardness on the inverse root of grain diameter for all materials which had reached full density. Figure 13 shows the dependence of yield strength on the same parameter. It should be noted that some of the highest compression strength samples broke before they clearly yielded. While

significant hardening and strengthening results from reducing the grain size, the magnitude of the effect is not as great as would be expected from a linear extrapolation of the large grain size material results into the nanoscale region, inspite of the additional strengthening from the oxide. This result agrees with the idea of Nieh and Wadsworth [11] that the Hall-Petch effect is overtaken at small grain sizes by other mechanisms that lead to lower the strength with decreasing grain size. Whether this phenomena, which was observed by many others[8,10,13], is intrinsic to fine grain sizes or the result of incomplete consolidation in their materials is not always clear in the literature. The results presented here in Figures 12 and 13 are taken from samples for which the hardness has peaked and the density has reached a plateau. These samples are believed to have reached full density. The nanograined materials, though extremely strong, are not as hard as would be predicted by a Hall-Petch fit to the properties of large grained material. It would be necessary to explore even finer grain sizes than those studied here to observe whether a softening with decreasing grain size actually occurs.

Conclusions

The uniqueness of bulk nanocrystalline materials is the small grain size. During the process of consolidation of these materials, the most important thing to preserve, at least partially, is the grain size. Ball-milled powder has an extremely small starting grain size. The size and hardness of the particles in ball-milled powder is such that processes like HIPing must be used to consolidate it effectively. Vapor condensed powder has extremely small particles that are not so hard and consolidation proceeds easily by sintering at relatively low temperatures. However, the resulting, fully dense body has lower hardness than, ball-milled material HIPed to full density. The hardness and the strength of both nanograined powders compacted bodies is substantially higher than these of regular powders. It seems that the oxides formed during consolidation might be an important governing the strength and microstructure of the compacted bodies.

The behavior of these nanoscale powders can be understood by considering the three most important processes taking place during the consolidation of any powder: densification, particle bonding, and grain growth. Optimization of these processes may result in unique mechanical properties of the ball milled powders. It was found that these three processes are strongly influenced by the grain size and particle size of the powders investigated, and oxidation level.

Acknowledgments

References

(1) H. Gleiter, "Nanocrystalline Materials," Progress in Materials Science 33 223-315 (1989).

2) Research Opportunities for Materials with Ultrafine Microstructures, National Materials Advisory Board Report No. 454 (1989).

3) R. D. Shull, First NIST Workshop on Nanostructured Material, National Institute of Standards and Technology Report No. NISTIR 5456 (1994).

(4) C. Suryanarayana, "Nanocrystalline Materials," International Materials Reviews 40 pp. 41-64, (1995).

(5) V. G. Gryaznov, M. Yu. Gutkin, A. E. Romanov, and L.I. Trusov, "On the Yield Stress of Nanocrystals," J. of Materials Science 28 4359-4365 (1993).

(6) W. Chen, A. Pechenik, S. J. Dapkunas, G. J. Piermarini, and S. Malghan, "Novel Equipment for the Study of the Compaction of Fine Powders," J. American Ceramic Society 77 1005-1010 (1994).

(7) M. P. Dariel, D. S. Lashmore, and M. Ratzker, "New Technology for Mercury Free Metallic Dental Restorative Alloys," Powder Metallurgy 37 p. 88 (1994).

(8) G. E. Fougere, J. R. Weertman, and R. W. Siegel, "Processing and Mechanical Behavior of Nanocrystalline Fe," Nanostructured Materials, 5 127-134 (1995).

(9) J.R. Groza, and R.J. Dowding, "Nanoparticulate materials densification" Nanostructured Materials Vol. 7 (1996) pp. 749-768.

10) J. R. Weertman, M. Niedzielka, and C. Youngdahl, "Hall-Petch Behavior in Nanocrystalline Metals," in Mechanical Properties and Deformation Behavior of Materials Having Ultra-Fine Micro-structures, edited by M. Nastasi, D. M. Parkin, and H. Gleiter, published by Kluwer Academic Publishers, Dordrecht (199?).

11) A. Munitz, Z. Livne, J. C. Rawers and R. J. Fields, "Cold Compaction of Nanograin Iron Alloys", to be published in Conf. Hawaii, 1996

12) T. G. Nieh and J. Wadsworth, "Hall-Petch Relation in Nanocrystalline Solids," Scripta Metallurgica et Materialia 25 955-958 (1991).

13) J. S. C. Jang and C. C. Koch, "The Hall-Petch Relationship in Nanocrystalline Iron Produced by Ball Milling," Scripta Metallurgica et Materialia 24 1599-1604 (1990).

List of Tables

List of Figures

Table 1. Characteristics of powders used in the present study.

Code	Powder Production Process	Particle Diameter [μm]	Grain Size [nm]	O +N Concentration [wt.%]	Tap Density [%]
NN	Evap/Cond	.15 ± .05	55 ± 25*	5.7% O	7.5±2.5
NM	Ball Mill	Bimodal 1.5 ± 0.5 .15 ± .05	6.5 ± 1.5*	1.9% N 2% O	36 ±2.5
MM(a)	Atomized	7 ± 1	>1000	<<1% O	40 ±2.5
MM(b)	Grinding	60 ± 10	>1000	<<1% O	43 ±2.5

* From X-ray analysis.

Table 2a: Behavior of consolidated NN powder. There is an uncertainty of about 5% in all the values.

Fracture Behavior (strain to Fracture)	compressive Max. (MPa)	compressive yield(MPa)	Hardness, H_V(Kg/mm^2)	Density (g/ml)	Processing History[a]
Failed on lathe (0%)	-	-	110	4.2	as CIPed
Failed on lathe (0%)	-	-	135	-	S[b]375C/24hrs
Cleaved	1400	1400	410	5.9	H₂[c]
Failed on lathe (0%)	-	-	440	6.3	S500C/3hrs
Cleaved	1800	1800	520	6.8	P[d]500C
Cleaved	1700	1700	680	6.3	H₂[c]-P500C
Cleaved	----	----	430	6.3	S580C
Shear fracture (2%)	1125	950	250	6.3	H₂[c]S585C/3hrs
Ductile Fe, Brittle Oxide (0.05%)	1200	1160	380	6.6	S700C/3hrs
Shear fracture (17%)	840	730	300	7.0	S850C/3hrs
Shear fracture (14%)	700	350	230	6.9	S300C/18hrs-S965C/3hrs
Ductile[e]	1500	280		7.5	H₂[c]S585C/3hrs -S965C/3hrs

(a) all the samples were first CIPed at 350 MPa, then processed as indicated
(b) S indicates sintered in vacuum of 1 Pa.
(c) H₂ indicates sintered in H₂ atmosphere at 375 °C for 24 hours.
(d) P indicates HIPed at pressure of 175 MPa for 3 hours.
(e) Did not fail by fracture, test stopped after excessive deformation. Therefore the value is meaningless and represent the fact that the sample is very ductile.

Table 2b: Behavior of consolidate NM powder. There is an uncertainty of about 5% to 10% in all the values.

Fracture Behavior (strain to Fracture)	compressive Max. (MPa)	compressive yield (MPa)	Hardness, Hv (kg/mm^2)	Density (g/mL)	Processing History[a]
Brittle fracture (0%)	---	---	120	4.6	as CIPed
Brittle fracture (0%)	---	---	120	4.6	S[b]370C
Brittle fracture (0%)	---	660	240	5.9	P[d]370C
Brittle fracture (0%)	---	---	120	4.65	S[b]500C
Brittle fracture (0%)	---	800	840	7.0	P[d]500C
Brittle fracture (0%)	---	---	120	4.7	S[b]580C
Brittle fracture (0%)	1200	1200	820	7.1	P[d]580C
Failed on lathe (0%)	---	---	---	---	H2[c]- S[b]585C/3hrs
Brittle fracture (1%)	---	110	120	4.94	S700C/18hrs
Brittle fracture (0%)	2100	2100	570	7.1	P700C
Brittle fracture (0%)	1560	1380	580	7.5	H2-P700C
Ductile fracture (15%)	330	160	140	5.38	S300C/1hrs-S850C/3hrs
Ductile Fe, Brittle Oxide (3%)	1390	1200	470	7.1	P850C
Ductile[e]	1700	110	160	7.0	S965C/120hrs
Ductile[e]	1000	610	300	6.9	P965C/3hrs

(a) all the samples were first CIPed at 350 MPa, then processed as indicated

(b) S indicates sintered in vacuum of 1 Pa.

(c) H2 indicates sintered in H2 atmosphere at 375 °C for 24 hours.

(d) P indicates HIPed at pressure of 175 MPa for 3 hours.

(e) Did not fail by fracture, test stopped after excessive deformation. Therefore the value is meaningless and represent the fact that the sample is very ductile.

Table 2c: Behavior of consolidate MM(a) powder. There is an uncertainty of about 5% to 10% in all the values.

(7%)	---	---	40	5.7	S[b]25C/18 hrs
(7%)	180	120	40	5.7	S[b]500C/18 hrs
Partial brittle(15%)	180	120	40	5.7	S580C/18 hrs
Ductile (55%)	400	150	54	6.1	S700C/18 hrs
Ductile[e]	1700	530	170	7.8	P[d] 700C
Ductile[e]	1500	225	80	7.6	S300C/1hrs-S850C/3hrs
Ductile[e]	1250	380	60	7.8	P850C
Ductile[e]	1700	120	60	6.8	S965C/120hrs

Table 2d: Behavior of consolidate MM(b) powder. There is an uncertainty of about 5% to 10% in all the values.

Ductile[e]	1100	100	50	6.8	S[b]300C/18hrs-S965C/4hrs
Ductile[e]	1700	100	40	6.5	S965C/120hrs

(a) all the samples were first CIPed at 350 MPa, then processed as indicated

(b) S indicates sintered in vacuum of 1 Pa.

(c) H₂ indicates sintered in H₂ atmosphere at 375 °C for 24 hours.

(d) P indicates HIPed at pressure of 175 MPa for 3 hours.

(e) Did not fail by fracture, test stopped after excessive deformation. Therefore the value is meaningless and represent the fact that the sample is very ductile.
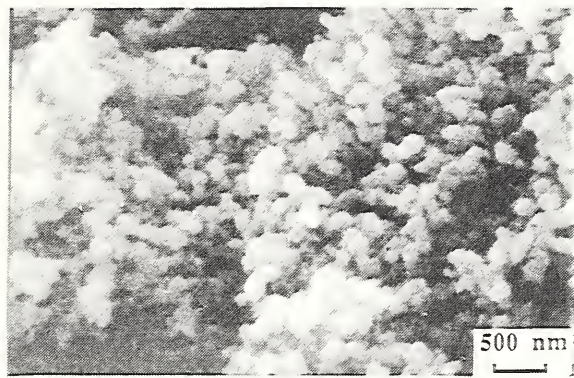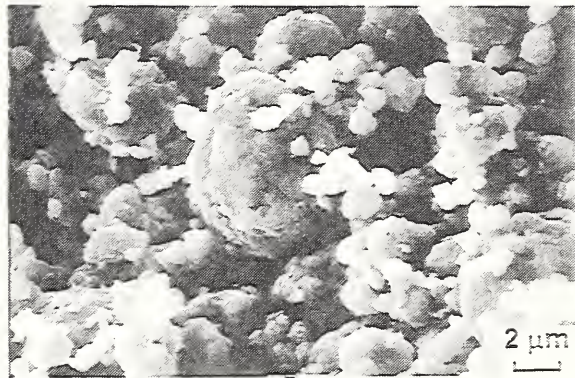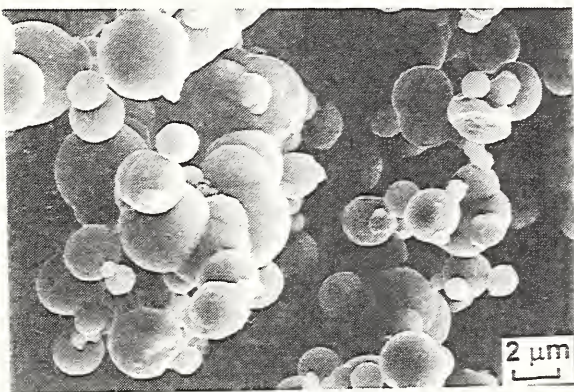
Figure 1. Morphology of the starting powders:(a) NN, (b) NM, (c) MM(a), and (d) MM(b).
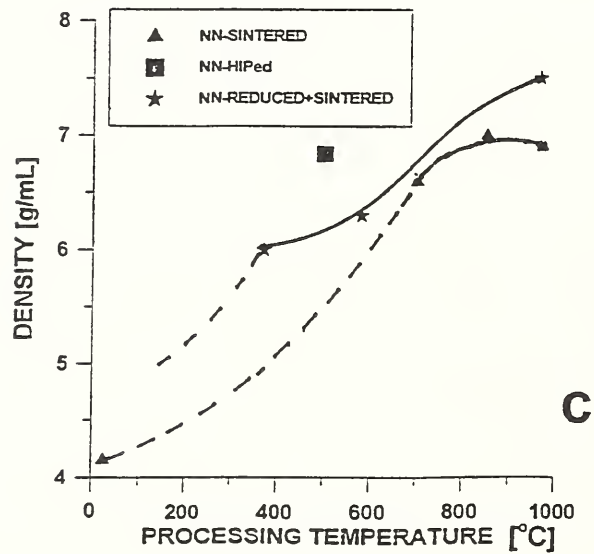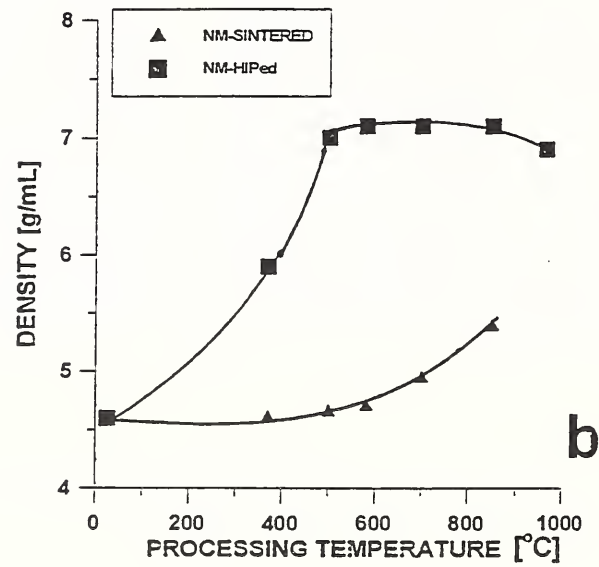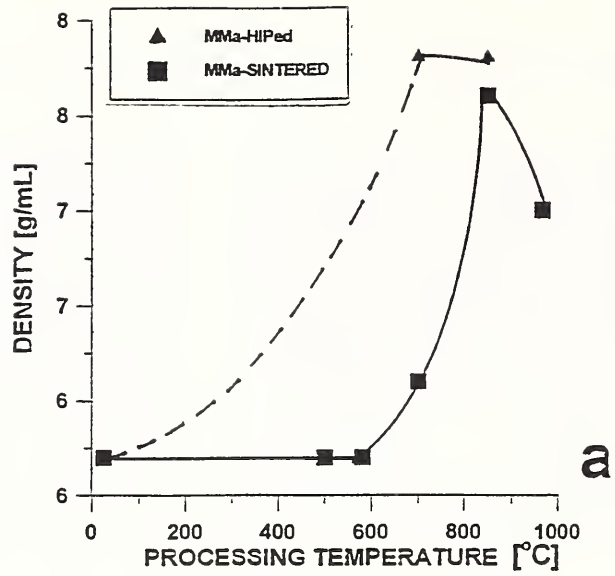
Figure 2. Density of compacts after CIPing, sintering, and HIPing starting with (a) MM powder,(b) NM powder, and(c) NN powder.
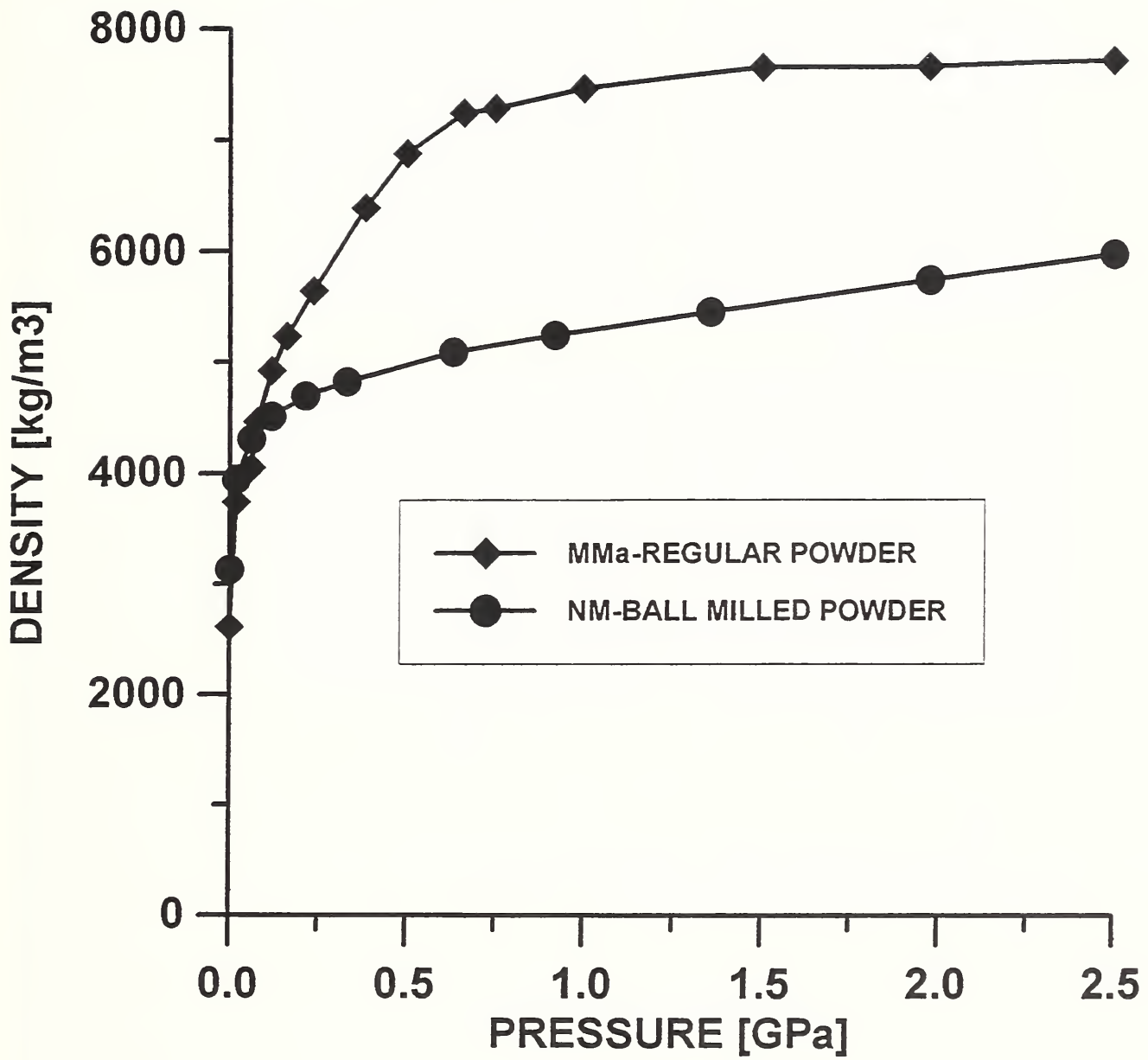
Figure 3. Density versus pressure in closed die compaction for two types of powder.
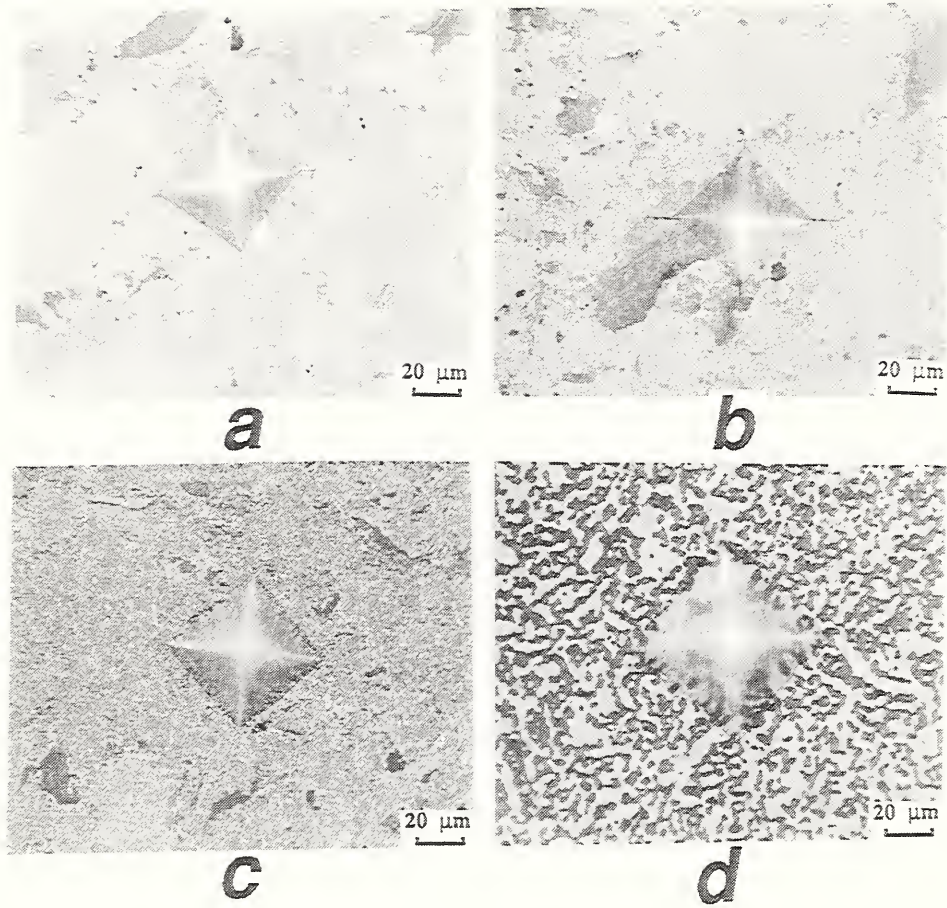
Figure 4. Examples of microstructures of consolidated NN powder sintered at (a) 500 °C, (b) 580 °C, (c) 700 °C, and (d) 965 °C.
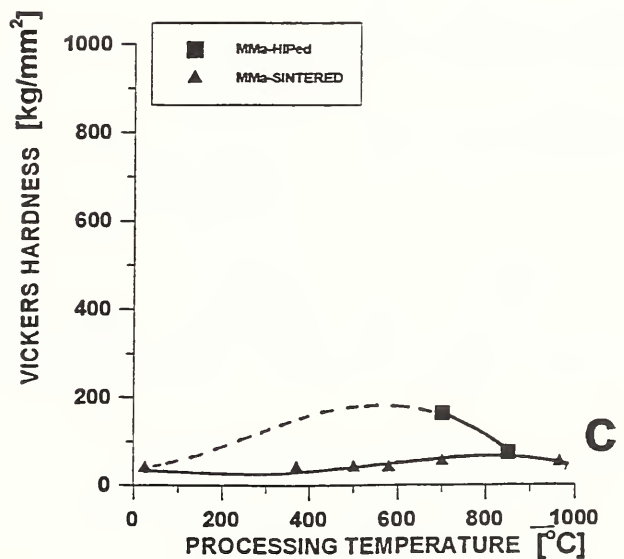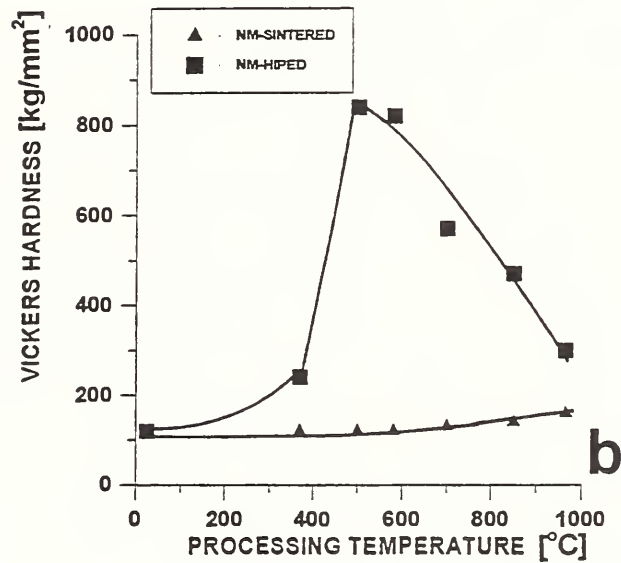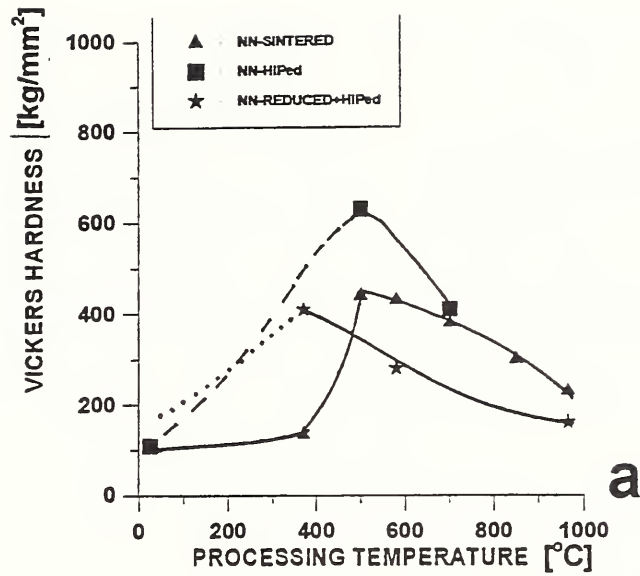
Figure 5. Hardness of compacts that were first CIPed, then sintered or HIPed at different temperatures.

(a)
Compression Stress [MPa]
Relative Displacement [dL/L₀]

1- R375 °C; 2- R375 °C+SIN 580 °C;
3- R375 °C+SIN 965 °C
4- HIP 500 °C; 5- SIN 850 °C

(b)
Compression Stress [MPa]
Relative Displacement [dL/L₀]

1- HIP 580 °C; 2- HIP 700 °C; 3- HIP 850 °C;
4- SIN 850 °C; 5- SIN 965 °C;

(c)
Compression Stress [MPa]
Relative Displacement [dL/L₀]

1- SIN 580 °C; 2- SIN 700 °C; 3- SIN 850 °C;
4- SIN 965 °C; 5- HIP 700 °C; 6- HIP 850 °C
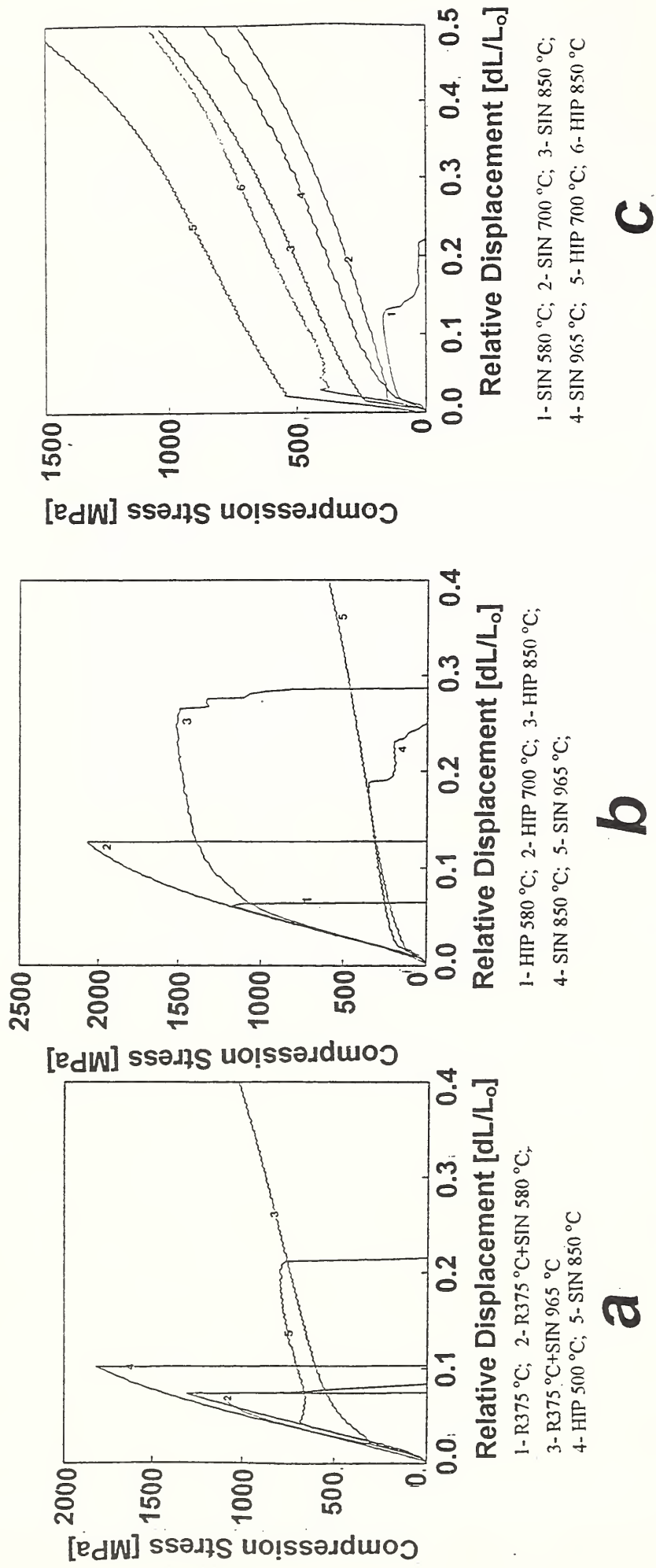
Figure 6. Selected stress-strain curves from compression tests on (a) NN, (b) NM,
and (c) MMa.
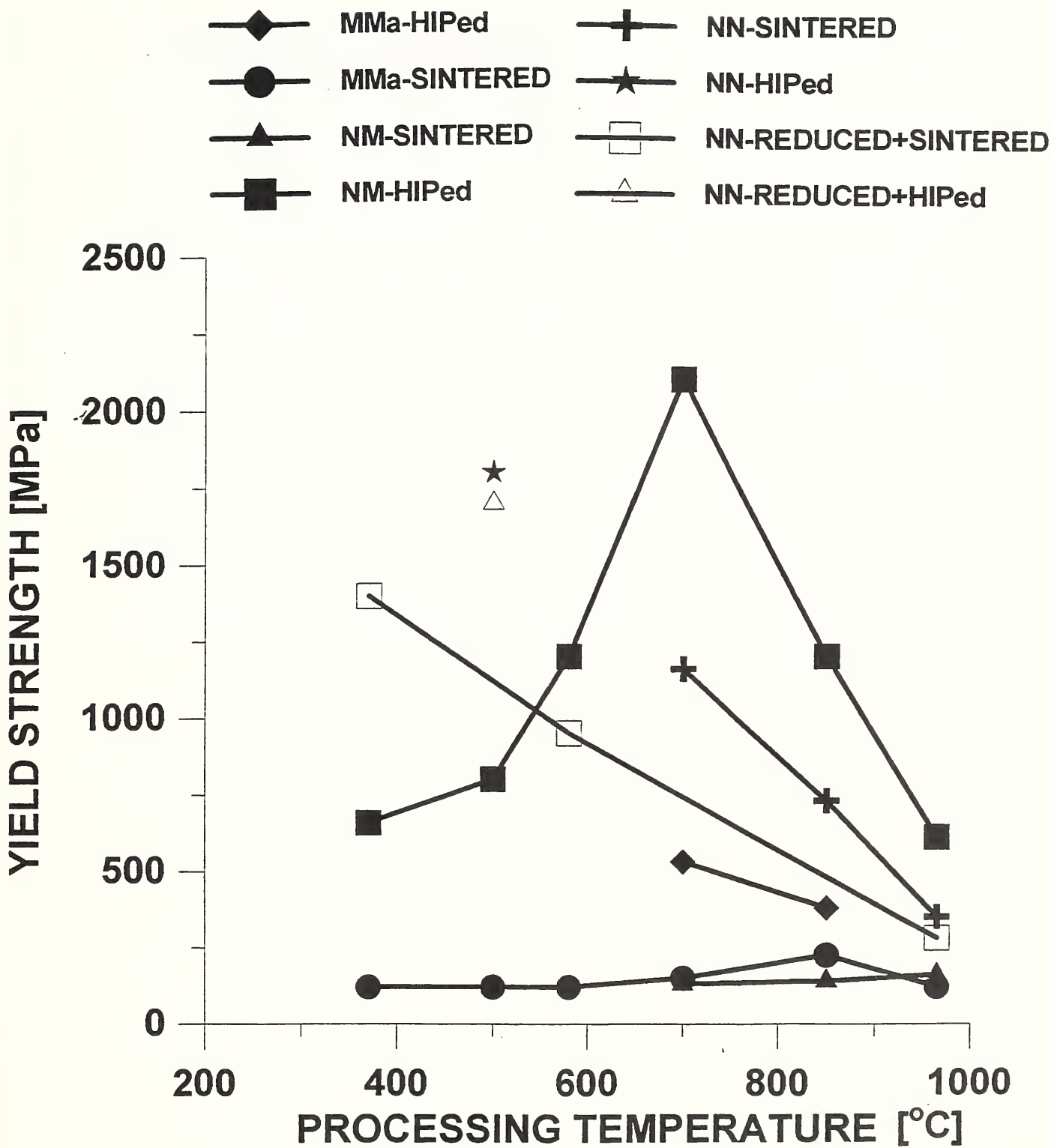
Figure 7. Compressive yield stress of NM compacts that were CIPed, sintered, or HIPed.

Figure 8. Fracture behavior of test cylinders: (a) ductile, (b) partially brittle, and (c) brittle.
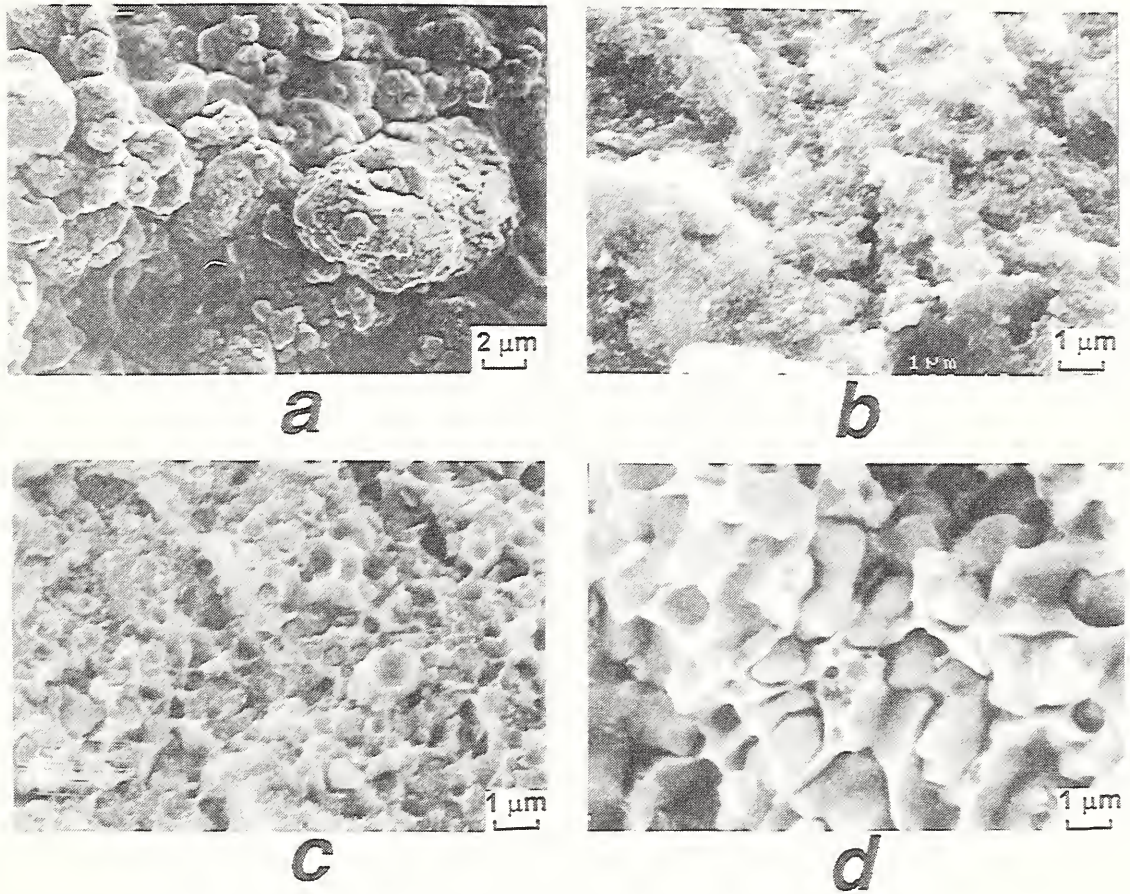
Figure 9. Fracture surfaces of NM after (a) sintering at 700 °C or HIPing at (b) 580 °C, (c) 700 °C, or (d) 850 °C.
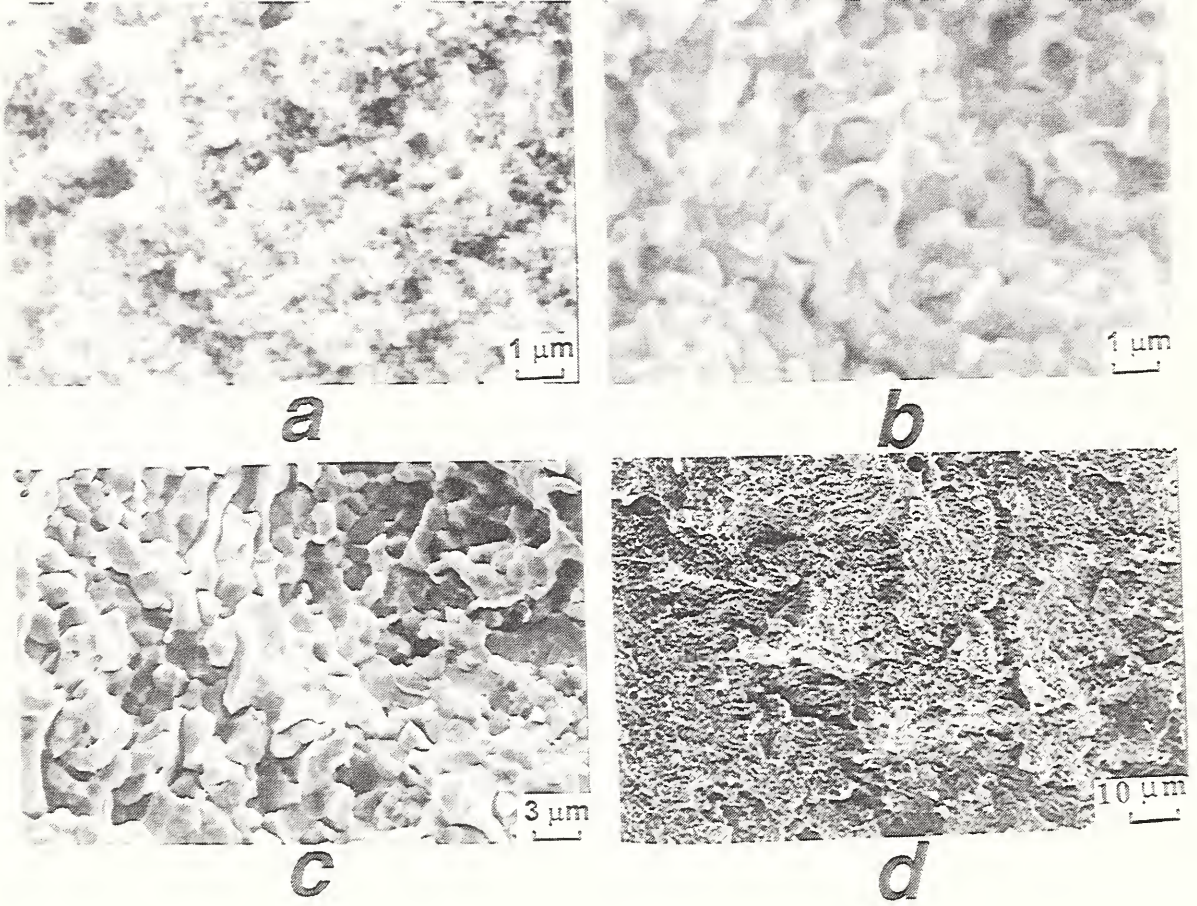
Figure 10. Fracture surfaces of NN after sintering at (a) 580 °C, (b) 700 °C, (c) 965 °C, or (d) HIPing at 500 °C.
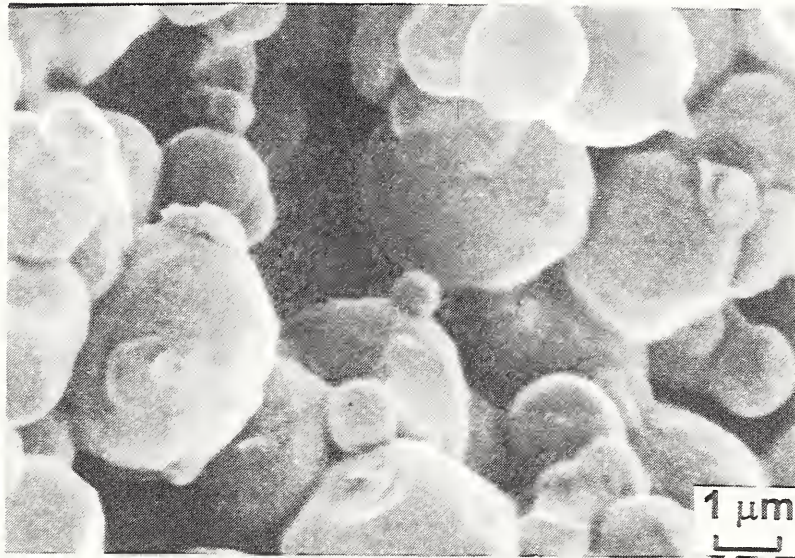
a
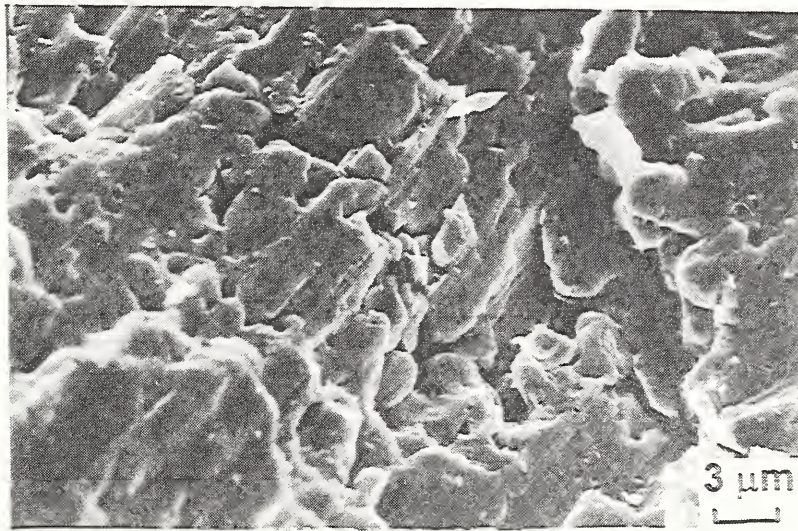
b

Figure 11. Fracture surfaces of MM(a) after sintering at (a) 580 °C and (b) 700 °C.
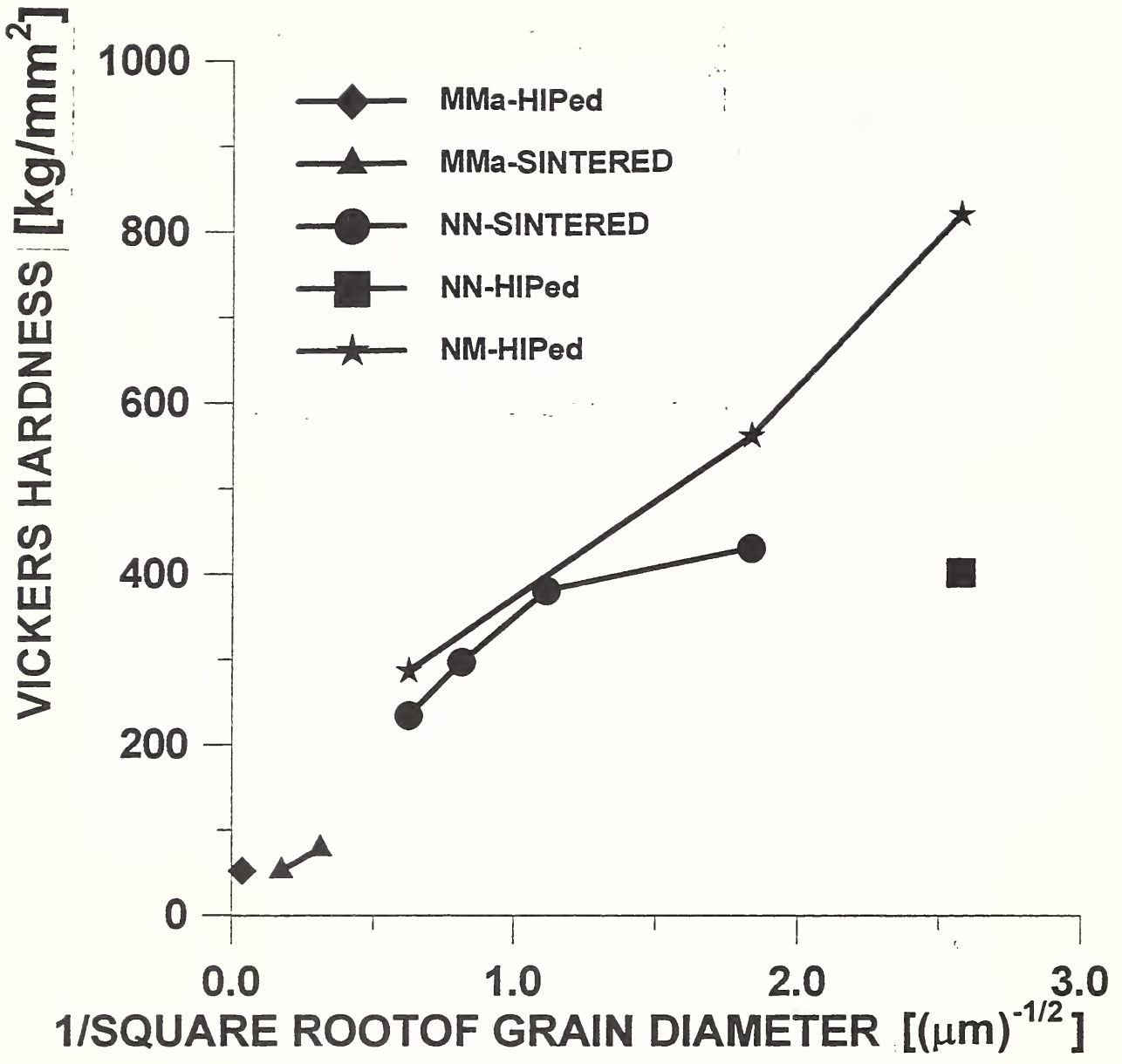
Figure 12. Hardness of iron as a function of grain size.
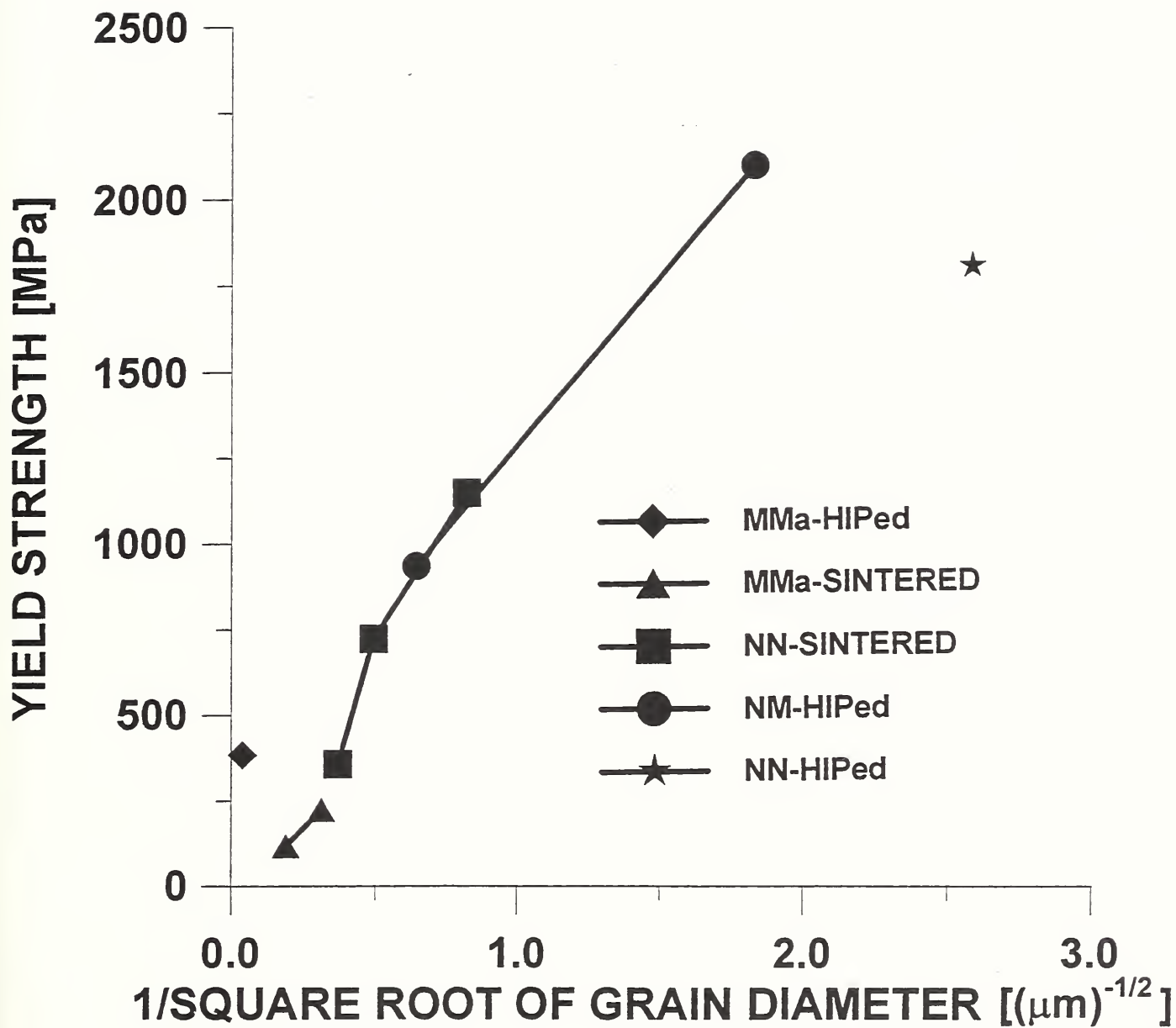
Figure 13. Yield strength of iron as a function of grain size.